Relativistic effects on the surface electronic structure of Mo(011)

K. Jeong, R. H. Gaylord, and S. D. Kevan
Department of Physics and Materials Science Institute, University of Oregon, Eugene, Oregon 97403
(Received 21 April 1988)

High-resolution photoemission studies of the Mo(011) surface have allowed us to isolate and to study the effects of the spin-orbit interaction on the surface electronic structure of Mo(011). We have observed and characterized three distinct phenomena, all related to the breaking of symmetry by the spin-orbit interaction. The first is a zone-center surface resonance which exists in a pseudogap between the bulk Γ_{8+} and the Γ_{7+} points, and is similar to one observed previously on W(011). We also have observed a surface state in a projected band gap opened by spin-orbit-induced hybridization between bulk bands at $\bar{N}$. Finally, we have observed avoided crossings of surface bands along the symmetry azimuths. These bands would be of opposite mirror-plane symmetry in the absence of the spin-orbit interaction, but hybridize under its influence. The transfer of both the polarization behavior and contamination sensitivity from one band to another is observed and characterized. We speculate on the relevance of these results to other surface properties, including reconstruction and work-function change.

I. INTRODUCTION

The characterization of nominally clean surface electronic structure continues to be a subject of considerable interest.[1-3] This in large part is due to the variety of important surface processes which it governs, including dipole layer formation and work-function determination, atomic reconstruction and relaxation, and chemical reactivity. The increasing precision of experimental and computational techniques continues to foster a better fundamental understanding of such phenomena. In particular, high-resolution angle-resolved photoemission (ARP) experiments have allowed increasingly subtle phenomena to be investigated. The primary purpose of this paper is to report accurate ARP studies of clean Mo(011) which illustrate significant perturbation of surface electronic structure by the spin-orbit interaction. This relativistic effect may play a significant role in determining other macroscopic and microscopic surface properties.

The broad interest in the electronic structure of W(001) and Mo(001) generated by their observed clean-surface reconstructions has not been transferred to the corresponding (011) surfaces.[4-15] The clean (001) reconstructions are thought to result from formation of zig-zag chains of surface atoms oriented along the [110] direction. Since bcc (011) surfaces are relatively close packed, it was generally believed that they were stable to reconstruction. However, the W(011) surface was recently observed to undergo a displacive "(1×1)" reconstruction upon adsorption of roughly half a monolayer of hydrogen.[16,17] The Mo(011) surface has not yet been observed to display similar behavior.[17] Subsequently, we presented evidence that at least part of the driving force for the W(011) reconstruction lay in hydrogen-induced changes in the surface electronic structure.[18] ARP studies will thus play an important role in understanding why W(011) reconstructs, and what distinguishes Mo(011) from W(011).

It is not yet certain that the displacive reconstruction does not occur on Mo(011), since the reconstruction must be oriented macroscopically by uncontrollable surface imperfections in order to be manifested by the symmetry observed in the low-energy electron-diffraction pattern.[16,17] The bulk electronic structures of tungsten and molybdenum are qualitatively similar. Given the similarity between the clean-surface reconstructions and some of the hydrogen-induced reconstructions observed on W(001) and Mo(001), one might expect the same (1×1) reconstruction to be observed on Mo(011) as on W(011). That it has not been observed is suggestive that the spin-orbit interaction may contribute to the instability of the (011) surfaces, since this effect is significantly larger in the $5d$ metal.

In order to understand the distinction between W(011) and Mo(011), we have initiated detailed studies of the clean and hydrogen-contaminated surface electronic structures. We report here our initial results on clean Mo(011). The surface electronic structure of Mo(011) has not been well studied either experimentally or computationally. The only angle-resolved photoemission study of which we are aware was undertaken 12 years ago, and was not particularly detailed.[6] The electronic structure calculations for this surface have been semiempirical and model dependent.[4,5] Relativistic effects were not considered.

The relative importance of the spin-orbit interaction in these metals can be estimated by comparing the atomic spin-orbit parameters [$\xi(4d)=0.12$ eV and $\xi(5d)=0.45$ eV in Mo and W, respectively][19] to a calculated or measured d-band width (roughly 1–2 eV).[20,21] On energetic grounds, we see that in molybdenum the spin-orbit interaction is small but not negligible compared to typical orbital hybridization energies, while in tungsten it is significantly more important. Its effect in molybdenum on some highly integrated observables, such as specific heat, total and local density of electron states, and trans-

port properties, might therefore not be particularly important. However, the spin-orbit interaction induces a lowered symmetry in the electronic states, a fact which can be have a pronounced effect on the electronic structure in localized regions of momentum space. Such effects are amenable to study using ARP.

In an ARP experiment the energy and momentum of an emitted photoelectron are measured simultaneously.[1-3] Using energy- and momentum-conservation relations, the quasiparticle dispersion relations can be extracted directly. Of particular interest in these studies are electronic levels exhibiting pronounced two-dimensional behavior, i.e., surface states and surface resonances. These gives a very good indication of the electrostatic potential that an electron experiences in the vicinity of a surface, and thus have direct relevance to studies of other surface properties. Surface states are pure states which exist in band gaps observed in projecting the bulk band structure along the surface normal. Surface resonances are impure surface states, i.e., states which are degenerate with bulk bands at the same momentum parallel to the surface and of the same symmetry.

With this perspective, the effects of the spin-orbit interaction on surface electronic structure can be easily predicted. For instance, bulk bands which are of differing symmetry neglecting the spin-orbit interaction and which can thus cross at some value of crystal momentum might be of the same lowered double-group symmetry when the spin-orbit interaction is included. The band crossing is then forbidden, and a new projected gap of width of order ξ can appear. Completely new surface states can thus exist purely due to the perturbing effects of the spin-orbit interaction. Alternatively, surface states in symmetry-projected band gaps can become resonances by virtue of weak spin-orbit-interaction-induced coupling to a bulk continuum which would otherwise have a different symmetry. If the spin-orbit interaction is large, these resonances could be so strongly coupled to bulk states that they would acquire an energy width comparable to that of the bulk band, thereby becoming indistinguishable from the bulk state. Thus, the inclusion of the spin-orbit interaction in a nonrelativistic or a scalar-relativistic calculation can, in principle, either create new surface states or destroy existing ones.

Unfortunately, these effects have not been well documented experimentally or theoretically. State of the art scalar-relativistic calculations of surface electronic structure push the limits of current computational capacity. In systems with inversion symmetry, inclusion of the spin-orbit interaction makes a real Hamiltonian matrix complex and doubles its size. In view of the success that scalar-relativistic calculations have had in predicting highly integrated quantities such as work function and total energy, there is at first little impetus to investigate what appear to be subtle effects arising from the spin-orbit interaction. Other approximations in the calculations such as a truncated basis set or consideration of too few atomic layers in a slab calculation normally take precedence in the decision of how to allocate computing power. An important exception to the neglect of the spin-orbit interaction in surface electronic structure calculations, however, was recently reported by Matthiess and Hamann and concerned W(001).[22] This calculation included the spin-orbit interaction in a partially self-consistent way. The authors concluded that bands near the Fermi level which apparently help to drive the clean surface to reconstruct are significantly perturbed by spin-orbit effects, and that these might play an important role in determining the observed geometric ground state for the surface. It thus appears that further experimentation is in order to characterize the general importance of spin-orbit effects on surface electronic structure.

In the absence of spin resolution and circularly polarized light, it is generally not a simple matter to extract the specific spin-orbit effects from ARP data. To date, there have been three experiments reporting the existence of spin-orbit-interaction-induced surface features.[23-25] These has arisen no simple, intuitive model for the occurrence and characteristics of these.[3] We show below that careful, high-resolution experiments can provide quite a detailed account of the various manifestations of the spin-orbit interaction. In Sec. II we explain our experimental procedures. Section III presents experimental results on Mo(011) and analyzes them in terms of the broken symmetry due to the spin-orbit interaction. Section IV speculates upon the ultimate significance and generality of our results.

II. EXPERIMENTAL TECHNIQUES

A 99.99%-purity Mo(011) crystal 1 cm in diameter was oriented normal to the [011] bulk crystalline axis by Laue x-ray backreflection to within $<0.5°$. A 1.5-mm-thick slice was cut and electromechanically polished in 15% sulfuric acid in methanol to a lustrous finish, and inserted into our vacuum system. After several cycles of oxidation at 1300–1500 K followed by sublimation of the oxide at 2300 K, an exceptionally clean and well-ordered surface was obtained as determined by low-energy electron diffraction and Auger-electron spectroscopy. The operating pressure of $(0.8-1.2)\times 10^{-10}$ torr was sufficient to maintain a clean surface for 15–20 min, as determined by the gradual disappearance of some of the more contamination-sensitive features in our spectra. These could easily be restored by thermally desorbing residual hydrogen and carbon monoxide from the surface. This desorption procedure could be performed repeatedly for several days without degradation of the surface.

Where required to determine the surface sensitivity of certain spectral features, the room-temperature surface was exposed to hydrogen gas in the form of H_2, either by backfilling the chamber or by placing the sample in the line of sight of a channel-plate-array doser.

The ARP experimental system has been described previously.[26,27] High angle- and energy-resolution experiments can be performed readily in this system. For the experiments described here, the total instrumental resolution was always less than 80 meV [full width at half maximum (FWHM)], and the full angular acceptance was 1° or better. Experiments were performed at the National Synchrotron Light Source, using a 6-m toroidal-grating

monochromator. Spectra could be accumulated with an adequate signal-to-noise ratio under these conditions in typically 2–5 min.

III. RESULTS AND DISCUSSION

The systematic studies reported here involved accumulating over 100 ARP spectra from the clean and adsorbate-contaminated surface. The experimental goal was to determine which spectral features could be associated with bulk states, which with surface states, and which with surface resonances. We followed the normal procedure in such experiments of initially determining which features were particularly sensitive to contamination. Those that passed this test were assumed conditionally to arise from electron states having significant amplitude in the surface layers, while those that did not were assumed to arise from bulk states which simply terminate at the surface. This is not a fail-proof test, and further studies are normally required for a definitive assignment. In order to ascertain whether a feature is a surface state or resonance, we also checked for lack of dispersion with the component of momentum normal to the surface, as would be expected for a two-dimensional state. Finally, the states which still appeared to be surface levels were compared with a projection of the calculated bulk band structure normal to the surface to determine whether they were associated with a band gap. This comparison with a calculated ground-state projection is not without problems, since photoemission inherently measures an excited state. We use the projections as useful guides in interpreting our data, and acknowledge some ambiguity in interpreting surface features lying close to the edge of a band gap. Those that lie in gaps were assigned as states, and those that were not were assigned as resonances.

The dispersion relation parallel to the surface of each identified surface feature was determined as accurately as possible. Before proceeding with a detailed description of our data and results, we show a summary in Fig. 1. This shows our experimental dispersion relations plotted on a projection of the molybdenum bulk band structure. The bands were calculated using a Slater-Koster three-center nonorthogonal tight-binding interpolation scheme fitted to an augmented-plane-wave band structure.[21] Lacking a fully-relativistic first-principles calculation, we modified the interpolation scheme to include the spin-orbit interaction as described elsewhere.[28] We approximate the spin-orbit interaction with an energy-independent spin-orbit parameter taken from atomic-energy-level tables.[19] If anything, this will underestimate the magnitude of the spin-orbit perturbations.[22] The Mo(011) surface is of $c2mm$ symmetry, and thus has two mirror planes. The lines in k space associated with these are labeled $\bar{\Sigma}$ and $\bar{\Delta}$ in the surface Brillouin zone in Fig. 1. We report dispersion relations measured in these planes. The inclusion of the spin-orbit interaction breaks the mirror-plane symmetry of the associated electronic states, so that separation of even- and odd-symmetry projections are not necessary in this figure. The observed surface levels can be conveniently classified into three categories: a zone-center surface resonance, a complex set of levels observed along the symmetry lines, and a zone-boundary surface state or resonance. Each of these categories is considered separately below.

A. Zone-center surface resonance

Recently, we reported the observation of a surface resonance on W(011) which exists in a projected "pseudogap" at the center of the surface Brillouin zone.[23] The data points in Fig. 1 near $\bar{\Gamma}$ at a binding energy of 1.22 ± 0.04 eV are ascribed to a similar resonance on Mo(011). The origin of the pseudogap is given in Fig. 2, which shows the relativistic bulk bands of molybdenum calculated using the modified interpolation scheme along the high-symmetry lines of the bulk Brillouin zone. The $\bar{\Gamma}$ point of the surface zone projects from the $\Gamma-N$ line of the bulk zone. The pseudogap exists at the Γ point between the spin-orbit-split Γ_{8+} and Γ_{7+} levels. We refer to this as a pseudogap because at momenta near the zone-boundary band three is degenerate with the gap. In the presence of the spin-orbit interaction, all bands along this line reduce to Σ_5 symmetry. A state located in the

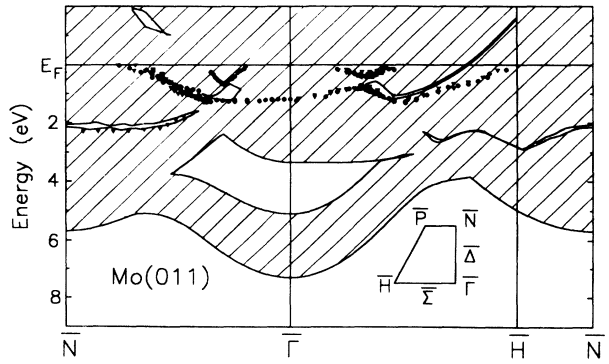

FIG. 1. Bulk molybdenum band structure projected onto the (011) surface Brillouin zone. The calculation includes the spin-orbit interaction, as explained in the text. The data were taken at the following photon energies: ●, $h\nu=24$ eV; △, $h\nu=40$ eV; ▽, $h\nu=50$ eV; □, $h\nu=60$ eV.

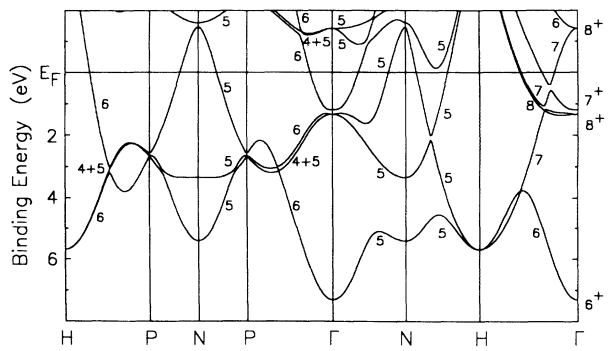

FIG. 2. Bulk molybdenum bands along the high-symmetry lines of the bulk Brillouin zone calculated using a nonorthogonal tight-binding interpolation scheme including the spin-orbit interaction, as explained in the text.

pseudogap must be coupled to the bulk continuum and would thus be identified as a resonance. This condition is manifested in Fig. 1 by the existence of the surface-resonance data in a shaded region.

The identification of this resonance in molybdenum is more difficult than it was in tungsten. This is because the spin-orbit parameter is larger in 5*d* than in 4*d* metals, leading to a larger calculated pseudogap in tungsten (0.59 eV) than in molybdenum (0.15 eV). As shown in Fig. 3, this leads to significant overlap between spectral features arising from the resonance and the nearby bulk states. Curves *a* and *b* in Fig. 3 show spectra of the clean and hydrogen-contaminated surface collected at normal emission using 24-eV photons. The emission near 1.0–1.5 eV binding energy relative to the Fermi energy E_F is clearly seen to arise from two overlapping features. The lower-binding-energy component is quite sensitive to contamination. This contamination-sensitive feature is in all respects similar to the resonance located on W(011).[23] In spite of the overlapping spectral features, careful studies have allowed us to connect this zone-center surface resonance with surface features observed along the symmetry lines. This will be explained further below.

Curves *c* and *d* were also collected at normal emission from the clean and contaminated surfaces, but at a photon energy of 40 eV. These spectra appear to present a different picture than spectra *a* and *b*. At $h\nu=40$ eV, only one feature is clearly apparent. This falls at nearly the same energy as the contamination-sensitive feature in curve *a*, but is not itself particularly sensitive to contamination. We interpret this result to the same cross-sectional effect described for the case of W(011).[23] At $h\nu=24$ eV, we sample states near the center of the bulk Brillouin zone in a simple direct-transition model using a plane-wave final state.[1–3] A state or resonance located in a zone-center gap would be expected to have its maximum intensity near this photon energy. In addition, the bulk states at the edge of the gap tend to lose intensity to the state or resonance under this condition. At $h\nu=40$ eV we would normally sample states near the zone boundary and the surface resonance would vanish. The observation of a nondispersive bulk feature nearly degenerate with the resonance must be ascribed to density-of-states emission from the bulk band edges. A similar approach is being used to interpret results from W(011).[29] As in that system, the location of the bulk features in our spectra of $h\nu=24$ eV has little to do with the energies of the edges of the pseudogap. The final three curves indicate the sensitivity of our spectra to the incident-photon polarization. As in tungsten, the resonance is not strongly excited with the polarization in the [011] mirror plane (curve *e*). Neglecting the spin-orbit interaction, this would require that the resonance be of Σ_1 or Σ_3 symmetry. Curves *f* and *g*, collected at photon incidence angles of 25° and 75° in the [100] mirror plane, respectively, indicate that the resonance is strongly mixed Σ_1 and Σ_3 symmetry since it does not vary appreciably in intensity relative to the nearby bulk features as the polarization is changed. Thus, as in W(011), the surface resonance has precisely the polarization character expected for a spin-orbit-interaction-induced feature. The nearby bulk features appear to be predominantly Σ_1 (lower) and Σ_3 (upper) symmetry, in line with expectations from the nonrelativistic bulk band structure.[20,21]

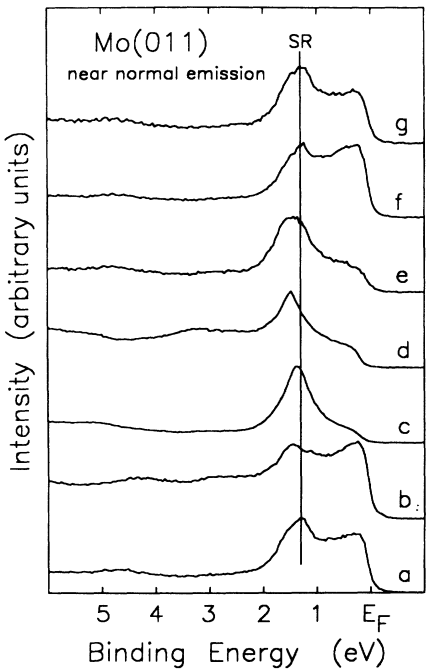

FIG. 3. Photoemission spectra of Mo(011) collected near normal emission. The vertical line labeled SR at $E_B=1.22\pm0.04$ eV indicates the spin-orbit-induced surface resonance. *a*, clean-surface spectrum collected at normal emission with 24-eV photons incident at 45°, with the polarization vector in the (011) mirror plane. *b*, same spectrum as in *a*, but following exposure to 0.3×10^{-6} torr sec of H_2. *c* and *d*, spectra similar to *a* and *b*, but collected at $h\nu=40$ eV. *e*, same spectrum as in *a*, but collected with the photon polarization vector in the (100) mirror plane. *f* and *g*, same spectra as in *a*, but with incidence angles of 25° and 75°, respectively.

It is interesting to note that even though the spin-orbit parameter of molybdenum is one-third that of tungsten, we still observe a fairly well-defined resonance. There are competing factors here: a smaller pseudogap will tend to decrease the likelihood of splitting off a state or resonance, but a smaller spin-orbit splitting would lead to a weaker coupling to degenerate bulk states and thus to a more well-defined resonance. We have not generated much intuition to guide our expectations, but we speculate that such resonances will occur fairly often.

B. Surface bands along the symmetry lines near E_F

The data in Fig. 1 also show several bands near the Fermi level along the $\bar{\Delta}$ and $\bar{\Sigma}$ lines of the surface zone which turn out to be strongly affected by the spin-orbit interaction. The behaviors along these two lines are distinct from one another, and we describe them in detail separately.

1. The $\bar{\Delta}$ line

The surface bands along $\bar{\Delta}$ are seen to exist primarily outside the vicinity of the gaps in the full-relativistic pro-

jection. They appear to avoid crossing in the vicinity of a small gap which, due to the figure's overall semblance to a face, we refer to as the $\bar{\Delta}$-eyeball gap. The spectra collected in this region of the surface Brillouin zone are among the most spectacular ever seen in condensed-state photoemission. This is shown in Fig. 4, where spectra collected near this gap at $h\nu=24$ are displayed. The photons were incident with mixed s and p polarization so that features of both odd and even mirror-plane symmetry will be observed. In order to understand the band dispersions at least qualitatively, we found it necessary to accumulate spectra at 0.25° (0.01 Å^{-1}) intervals as shown. This corresponds to a momentum increment of about 0.5% of the width of the Brillouin zone. The significant spectral variation in these intervals is observed over a region of ≈ 0.3 Å^{-1}. The momentum resolution used in accumulating these spectra was 0.03 Å^{-1}, full width at half maximum. This implies that, if enough signal were available to utilize even better resolution, we might see even more dramatic variations than those shown in the figure. Clearly, in regions such as this the typical momentum resolution of ≥ 0.1 Å^{-1} will miss some important physics.

Spectral features arising from both the upper (S_1) and lower (S_2) surface bands along $\bar{\Delta}$ can be seen in the Fig. 4. S_1 crosses E_F at $k_{\parallel}\approx 0.25$ Å^{-1}, disperses to higher binding energy at higher momentum to become degenerate with a bulk feature, and then disperses quickly back above E_F at $k_{\parallel}\approx 0.55$ Å^{-1}. This behavior is reflected in the bands shown in Fig. 1. For $k_{\parallel}<0.6$ Å^{-1}, S_2 appears as a low-binding-energy shoulder on a bulk feature bound by ≈ 1.5 eV. Further out in the zone, S_2 is seen to disperse to lower binding energy and eventually to cross E_F at $k_{\parallel}\approx 1.0$ Å^{-1}. S_1 and S_2 never cross, in accord with the data in Fig. 1.

The contamination sensitivity of these features is shown more clearly in Fig. 5, where selected spectra of the clean and contaminated surfaces are shown. Near the zone center (curves a and b), S_1 is above E_F, but S_2 is observed to be strongly attenuated following exposure to hydrogen. At $k_{\parallel}=0.39$ Å^{-1}, S_1 is observed at $E_B=0.53\pm 0.03$ eV on the clean surface (Fig. 5, curve c), but vanishes upon hydrogen adsorption (curve d). At this momentum, S_2 loses some intensity and shifts to higher binding energy to become degenerate with a bulk feature upon exposure. For our purposes, we take this shifting behavior to be indicative of surface localization in the same way as complete disappearance. This behavior can be seen more clearly at $k_{\parallel}=0.65$ Å^{-1} (Fig. 5, curves e and f). S_1 is again above E_F, but S_2 is observed simply to shift by 0.1–0.2 eV upon hydrogen exposure, while not losing much intensity at all.

In order to understand the origin of these surface

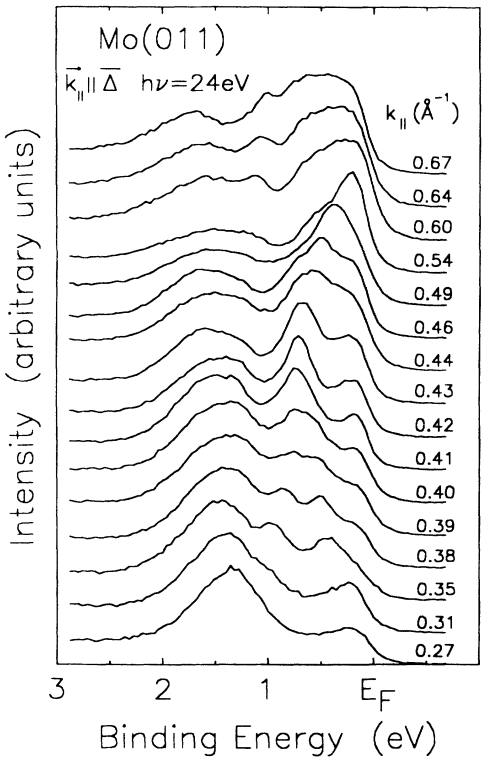

FIG. 4. Spectra of the clean Mo(011) surface collected near the $\bar{\Delta}$-eyeball gap at $h\nu=24$ eV. Photons were incident at 45° in the (011) mirror plane, while electrons were collected in the perpendicular (100) mirror plane.

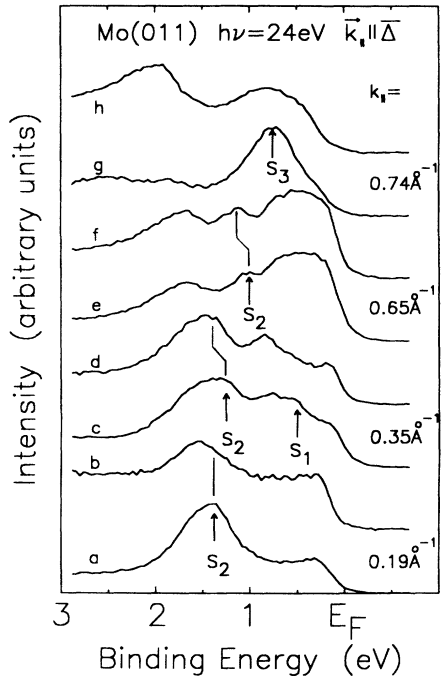

FIG. 5. Pairs of spectra collected in the $\bar{\Delta}$ azimuth from the clean and hydrogen-contaminated surface as a function of parallel momentum. a and b, spectra collected on the zone-center side of the eyeball gap. Note the disappearance of S_2 upon contamination (curve b). c and d, spectra collected near the eyeball gap, showing the sensitivity of both S_1 and S_2 to hydrogen. e and f, spectra collected on the zone-boundary side of the eyeball gap. Note that S_2 now shifts by ≈ 0.2 eV upon hydrogen exposure. g and h, spectra collected near the same parallel momentum as e and f, but in rotating the emission direction away from rather than toward the photon polarization direction. Note that S_3 is quite intense in this polarization and is observed to be very sensitive to hydrogen adsorption.

bands and their interaction in the eyeball gap, we project the bulk bands neglecting the spin-orbit interaction. In this case, the odd-even mirror-plane symmetry is retained. The projections of the odd and even manifolds are shown in Figs. 6(a) and 6(b), respectively, along with our experimental results. The $\bar{\Delta}$-eyeball gap in Fig. 1 is seen to result essentially from the intersection of projected gaps of odd and even symmetry. These projections provide a logical interpretation for the existence of S_1 and S_2. Near $\bar{\Gamma}$, S_1 exists in or near the even projected gap, while S_2 is in the odd gap. On the other side of the eyeball, these assignments are reversed. Apparently, the bands change their identity in the vicinity of the eyeball. Within the eyeball, the bands approach one another to within 0.50±0.04 eV, or about 4 times the spin-orbit parameter. This is what is expected if odd- and even-symmetry bands are allowed to hybridize under the influence of the symmetry-breaking spin-orbit interaction. The precise magnitude of the observed gap will provide valuable input to surface computations which include the spin-orbit interaction in d levels since the dominance of the atomic spin-orbit parameter will be modified by band-hybridization effects as well as by the spatial overlap between odd and even wave functions. As discussed in the Introduction, outside the eyeball gap, the bands are actually resonances by virtue of spin-orbit-interaction-induced coupling to the bulk continuum of the other single group symmetry. This coupling must not be particularly strong since the observed linewidths in our spectra are not significantly broader outside the eyeball gap.

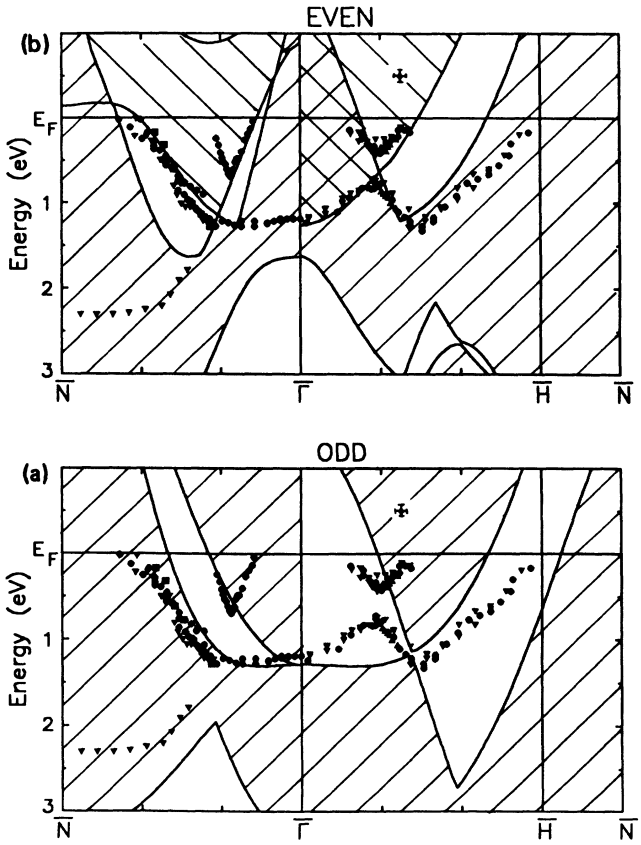

FIG. 6. Projection of the even and odd bulk molybdenum bands onto the (011) surface plane neglecting the spin-orbit interaction. The experimental points plotted on both the odd and even projections are the same as those shown in Fig. 1. Typical experimental uncertainty is indicated by the points located above the Fermi level.

This interpretation provides further predictions concerning the behavior of our spectral features. In the vicinity of an avoided crossing, the character of the eigenstates will interchange. The most obvious manifestation of this will be observed in the residual polarization dependences of the spectral features. Near $\bar{\Gamma}$, S_2 should mimic a state of odd-mirror-plane symmetry. On the other side of the eyeball gap, the state should behave as if it were predominantly of even symmetry. This switching of apparent symmetry should occur smoothly within the eyeball gap. This is, in fact, observed. The spectrum shown in curve e of Fig. 3, taken at normal emission, samples primarily the even-symmetry states for this mirror plane since the polarization vector is in the $\bar{\Delta}$ mirror plane. S_2, which connects smoothly to the zone-center surface resonance, is not observed. As we move out into the zone in this even polarization, the intensity of S_2 "turns on" near the eyeball gap and at some photon energies becomes a dominant feature in the spectrum. It has thus switched its polarization behavior in going through the eyeball gap in the way predicted above. The similar but inverted behavior expected for S_1 is difficult to observe since the band is apparently always within the hybridization region below E_F.

A more subtle prediction about the switching character of S_1 and S_2 concerns their behavior upon contamination of the surface. Near $\bar{\Gamma}$, S_2 is clearly quenched by hydrogen adsorption (curves a and b of Fig. 5). Similar to the above polarization dependence, this behavior is observable out to $k_{\parallel}=0.25$ Å^{-1}. The sensitivity becomes ambiguous through the eyeball gap (curves c and d of Fig. 5). On the zone-boundary side of the gap, the feature S_2 merely shifts downward by 0.1–0.2 eV after adsorption of hydrogen (curves e and f of Fig. 5). As for the polarization dependence, the opposite behavior for S_1 is difficult to observe due to this band's limited dispersion below E_F. However, as expected, just before the feature crosses the Fermi level on the zone-center side of the eyeball, there is a marked decrease in sensitivity to hydrogen exposure. Both the disappearance and the coverage-dependent shift are indicative of significant surface amplitude. The orbital character has clearly been transferred from one band to the other in traversing the eyeball gap.

A closer examination of our data near where S_2 crosses the Fermi level indicates that there is actually a third surface band along $\bar{\Delta}$. The apparent scatter of our data points in this region is one indication of this; there appear to be two Fermi-level crossings, one at $k_{\parallel}=0.93\pm0.05$ Å^{-1} and another at $k_{\parallel}=1.08\pm0.05$ Å^{-1}. The latter of these crossings corresponds to S_2 discussed above. The former, now called S_3, has a dispersion relation which is nearly degenerate with S_2 from E_F down to near the eyeball, where the S_3 band curves upward slightly before the

feature disappears from our spectra. S_2 and S_3 cannot be seen in the same spectrum taken along the $\bar{\Delta}$ symmetry axis, in part due to this degeneracy and in part due to a radically different behavior upon changes in photon polarization. Both S_2 and S_3 are nominally of even symmetry beyond the eyeball. However, S_3 has vanishingly small intensity when rotating the emission direction in plane toward the polarization vector, while it has a very large intensity rotating in the opposite direction. S_2 exhibits exactly the opposite behavior. This is shown in curves *g* and *h* of Fig. 5, which were collected from the clean and hydrogen-contaminated surfaces at a parallel momentum near that of spectra *e* and *f*, but accessed by rotating away from the polarization vector. S_3 is clearly visible in curves *g* and *h* but not *e* and *f*. Such an observed intensity asymmetry is fairly common in ARP, and has been explained qualitatively elsewhere.[30] Unlike S_2 on this side of the eyeball, S_3 is seen to be quenched by hydrogen adsorption. These two differing behaviors allow accurate and independent dispersion relations to be measured for S_2 and S_3. Complete Fermi surfaces for these two crossings can be measured, lending further credence to our analysis.[31]

2. *The $\bar{\Sigma}$ line*

As seen in Fig. 1, there are two surface bands along $\bar{\Sigma}$ which exist substantially outside the limits in Fig. 1 of what we call the Σ-eyeball gap. These appear to hybridize in this gap, but the details of the hybridization are substantially different in this case from that observed along $\bar{\Delta}$. The spectra accumulated near the $\bar{\Sigma}$-eyeball gap at $h\nu=50$ eV using in-plane *p* polarization shown in Fig. 7 are seen to be less complicated than those shown in Fig. 5. The two features labeled S_4 and S_5 are observed to disperse together and then apart. The unusual result observed is that on the $\bar{\Gamma}$ side of the gap the lower-binding-energy feature (S_4) is quite sensitive to contamination, while the higher-binding-energy feature (S_5) is not. On the other side of the eyeball gap, this sensitivity is inverted. In the transition region, we again needed to accumulate spectra at 0.25° intervals to characterize this switching accurately. This rapid switching is demonstrated by Fig. 8, which shows spectra of the hydrogen-contaminated surface in the vicinity if the eyeball. In these spectra, we see just one band which disperses smoothly upward for increasing momenta. Essentially, the part of S_4 toward the zone center and the part of S_5 toward the zone boundary have been quenched, while the other portions of these two bands merge to form a band which is shifted by 0.1–0.2 eV. Comparison of Figs. 7 and 8 indicates that the hydrogen-contamination sensitivity switches from S_4 to S_5 over a very narrow momentum range.

The effects shown in Figs. 7 and 8 again appear to be related to an avoided crossing between bands which, in the absence of the spin-orbit interaction, would be of different mirror-plane symmetries. The interpretation of this effect in terms of the symmetry-projected bands in Fig. 6 is somewhat different from the states along $\bar{\Delta}$. Near $\bar{\Gamma}$, both states S_4 and S_5 in Fig. 7 appear to exist in an odd-projected gap. The switching of surface character

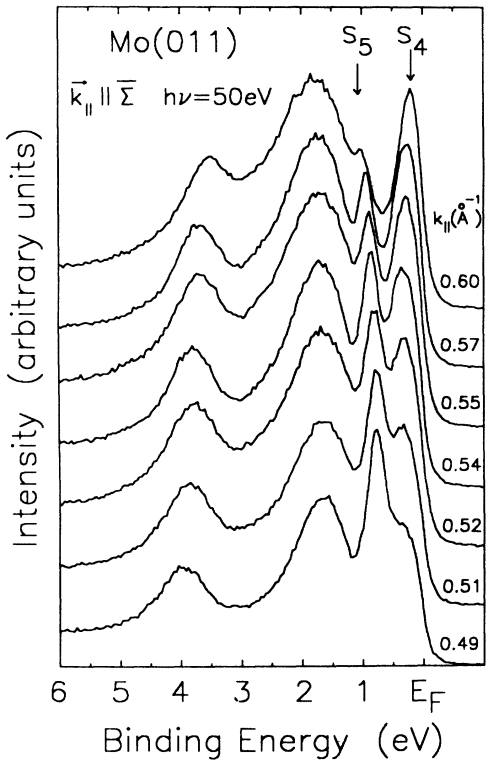

FIG. 7. Spectra of the clean Mo(011) surface collected near the $\bar{\Sigma}$-eyeball gap at $h\nu=50$ eV. Photons were incident at 45° in the (011) mirror plane and electrons were collected in the same plane.

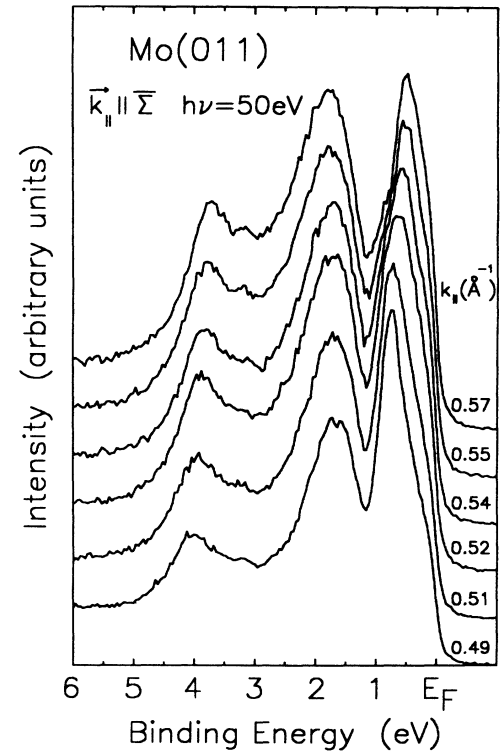

FIG. 8. Spectra collected in the $\bar{\Sigma}$ azimuth from hydrogen-contaminated surface as a function of parallel momentum. Note the disappearance upon contamination of S_4 from Fig. 7 in spectra collected on the zone-center side of the eyeball gap, while S_5 is extinguished in spectra collected on the zone-boundary side.

occurs near where S_4 disperses into the odd bulk continuum. At larger momentum, S_4 is near an even-projected gap, but does not appear to lie within it. The results shown in Fig. 7, accumulated in a geometry which would sample even states, are consistent with S_4 being primarily of odd symmetry near $\bar{\Gamma}$, but of even character on the other side of the eyeball. The polarization dependence indicates the inverted character for S_5, even though it appears to lie in an odd-projected gap on the $\bar{\Gamma}$ side of the eyeball. This enigma is explained by the "embedded" band edges shown in even projection of Fig. 6. These strongly suggest that the portions of S_5 close to the zone center and S_4 beyond the eyeball are associated with an even band edge which is embedded in an even continuum near $\bar{\Gamma}$. The sensitivity of S_4 to contamination by hydrogen is minimal for $k_{\parallel} > 0.5$ Å^{-1}. Beyond $k_{\parallel} = 0.5$ Å^{-1}, the lower band, S_5, adopts contamination-sensitive character and disperses into and through the eyeball gap. In the eyeball, S_5 exhibits a mixed symmetry which appears to depend upon photon energy and incidence angle. For $k_{\parallel} > 0.7$ Å^{-1}, S_5 once again appears to lie within the odd-projected gap and is preferentially excited by odd polarization. S_5 appears to disperse through a narrow section of the odd-symmetry projection near the center of the zone. In the vicinity of the $\bar{\Sigma}$ eyeball S_4 and S_5 approach one another to within 0.36±0.4 eV, again comparable to the atomic Mo(4d) spin-orbit parameter. As was observed along $\bar{\Delta}$, their sensitivity to contamination changes radically in the hybridization region, with the band exhibiting odd-polarization character, tending to be more sensitive to hydrogen.

Along $\bar{\Sigma}$, the bands which simply shift upon hydrogen exposure (S_4 away from $\bar{\Gamma}$ or S_5 near it) do so to a less degree than along $\bar{\Delta}$. Thus, in our spectra they have characteristics somewhat ambiguous in terms of assigning them as bulk or surface states. They do not disperse with normal momentum, however, and (see Fig. 8) do shift slightly upon either hydrogen or oxygen adsorption. From a theoretical point of view, it is difficult to understand how a surface band could become a pure bulk band simply by hybridization over a narrow (0.03–0.04 Å^{-1}) range of momentum with no observed change in linewidth or shape and no change in extrapolated dispersion relation. Indeed, the most unusual result is the precision with which S_5 appears to connect with the zone-center surface resonance (Sec. III A). The data points in Figs. 1 and 6 along $\bar{\Sigma}$ near the zone center were primarily collected at $h\nu = 40$–50 eV, in a geometry using mixed polarization. At this energy, however, the intensity in the resonance is dominated by the nearby bulk feature (curves c and d of Fig. 3). At $h\nu = 24$ eV, the resonance loses its intensity rapidly away from the zone center. S_5 then becomes weakly visible as the eyeball is approached. For now, we assign S_4 and S_5 to surface levels throughout their dispersions below E_F. Further theoretical work will help to understand these unusual results.

C. Zone boundary surface state

The final aspect of this surface's electronic structure which appears to be determined by the spin-orbit interaction is observed along the $\bar{\Delta}$ line near the zone boundary $\bar{N}$. The results in Fig. 1 show a surface band energetically very close to a narrow projected gap in this region roughly 2.3 eV below the Fermi level. Given the accuracy of the calculation and the uncertainties inherent in comparing a ground-state calculation with an excited-state spectroscopy, we feel that this surface band is actually a state residing within the projected gap. Indeed, other band calculations move this gap around so as to make this conclusion more or less the case.

The source of the projected gap at N can be determined from the bulk bands plotted in Fig. 2. The N point projects from the N–H line of the bulk Brillouin zone. Along this line, we observe a narrow projected gap opened by the spin-orbit interaction at a binding energy of ≈2.2 eV. In other words, in the absence of this perturbation, bands 2 and 3 along N–H would be of opposite mirror-plane symmetry. Introduction of spin forces them to hybridize, opening a gap of width of order $\xi(4d)$. Since we have attributed the surface state to this gap, its existence is clearly tied to the spin-orbit interaction.

Spectra of this band at $h\nu = 40$ eV as a function of parallel momentum of the emitted electron are shown in Fig. 9. The observed feature, labeled S_6, has several unusual characteristics. First, its intensity becomes quite small near $\bar{N}$ ($k_{\parallel} = 1.42$ Å^{-1}). The reasons for this are not clear at present. In addition, near $\bar{N}$, the observed line shape is very unusual. This may be due to the presence of nearby bulk features arising from the bulk band

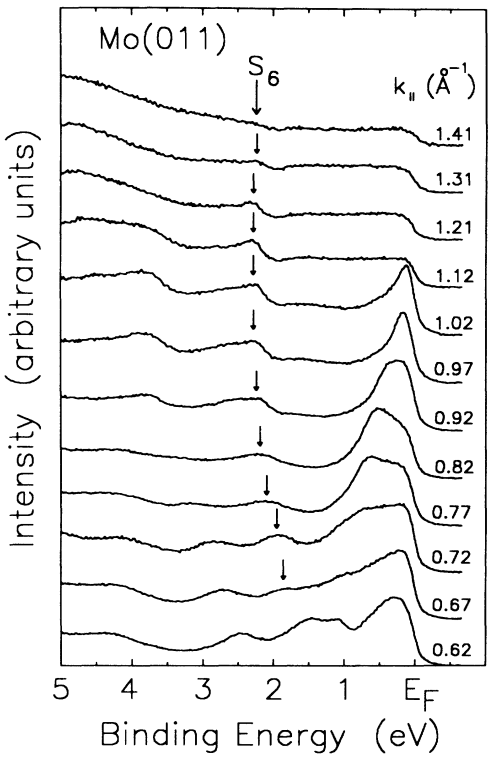

FIG. 9. Spectra of the clean Mo(011) surface collected at $h\nu = 40$ eV in the $\bar{\Delta}$ azimuth. The feature labeled S_6 is the surface state lying in a spin-orbit-induced projected band gap.

edges. Further from N, the state is observed to follow the gap, dispersing upwards slightly. The state disappears from our spectra near the $\bar{\Delta}$-eyeball gap when its own gap pinches off. The contamination sensitivity of this feature can be seen in the bottom spectrum of Fig. 10. It is one of the more hydrogen-sensitive features we have observed on this surface.

A final feature of interest concerning this state is the photon-energy dependence of its emission intensity. This is shown in the upper nine spectra of Fig. 10, where we show spectra collected at $k_{\parallel}=1.02$ Å^{-1} as a function of photon energy. In analogy with several other experiments on simpler systems, its location in a narrow hybridization band gap and its consequent close proximity to both band edges implies that the state is probably not very localized near the surface.[32–34] Indeed, using effective-mass theory, we can estimate a lower limit on its decay length into the bulk of >30 Å^{-1}.[35] Under these circumstances, we anticipate that the state will be observable over the narrow range of final momenta normal to the surface where the final-state wave function adequately matches that of the surface state.[32–34] The fact that the state is observed over a narrow range of photon energies is consistent with this expectation. Indeed, since the decay length of the surface state is probably longer than the probing depth of ARP for this material (≈ 5), the photon-energy dependence of the emission intensity is governed primarily by the final-state electron inverse lifetime.[32] This prediction is qualitatively confirmed by the data in Fig. 10, where the state is observable over a range of ≈ 5 eV.

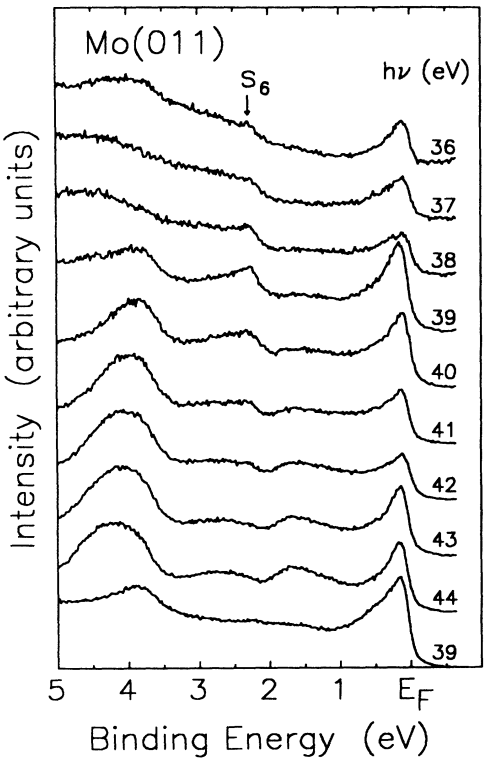

FIG. 10. Spectra collected at $k_{\parallel}=1.02$ Å^{-1} in the $\bar{\Delta}$ azimuth. Bottom spectrum was taken at $h\nu=39$ eV following a small dose of hydrogen, and the sensitivity of S_6 is apparent. The other spectra were collected at the various photon energies shown and show that the surface state maximizes in intensity near $h\nu=39$ eV.

The state is observed to maximize in intensity at $h\nu\approx 39$ eV. More importantly, using a simple free-electron final state,[1–3] this photon energy would correspond to a final-state momentum normal to the surface of ≈ 3.3 Å^{-1}. Roughly speaking, at $h\nu=39$ eV we sample bulk states about 30–40% of the way from N to H, or precisely where the spin-orbit gap is located. This is precisely the behavior one would expect for a surface state existing in a band gap opened by band hybridization, and gives some very important information concerning the wave function for the surface state.[32]

IV. SUMMARY AND CONCLUSIONS

A. Existence and character of surface localized states

It is useful at this point to summarize what we have learned, how it can be applied to develop predictive power in other systems, and what its ultimate significance might be in understanding phenomena of current interest in the study of nominally clean surfaces. What we understand and have documented fairly well is the effects of the spin-orbit-interaction-induced destruction of mirror-plane symmetry in bulk and surface electronic levels. Currently, one can generally predict, either by guessing, by using empirical models, or by doing sophisticated but nonrelativistic calculations, the existence and properties of surface states on metal surfaces in symmetry-projected gaps. Given this, the introduction of the spin-orbit interaction will simply require that bands of the same lowered symmetry not cross. By doing a fairly simple interpolation calculation of the sort used here, we can predict where in the surface zone the hybridization will occur. Moreover, to a fairly good approximation, the magnitude of the interaction can be estimated using atomic data.

Surface states may also become resonances by virtue of spin-orbit-induced coupling to a bulk continuum. Indeed, this effect has been justifiably neglected in studies of $3d$ metals where the spin-orbit interaction is small. In this $4d$ metal the spin-orbit-induced resonant coupling to bulk states appears not to be particularly important, since linewidths are not systematically larger away from the eyeball gaps. It will be interesting to compare other $4d$ and $5d$ metals in a systematic fashion.

We have significantly less predictive power concerning the *existence* of surface states and resonances existing in band gaps opened by the spin-orbit interaction. We have shown two such features in this paper, the zone-center resonance and the zone-boundary state, and there are three other reported in the literature.[23–25] Further extensions of the simple, empirical models[35–38] for surface-state existence to include the spin-orbit interaction might provide useful, predictive power. On the other hand, once the existence of such a state has been established, it appears that useful predictions of its characteristics can be made, for instance, using effective-mass theory. The

photon-energy using dependence of the Γ resonance and the N state are examples of this simple predictive power which tells us some qualitative yet useful information about these states' wave functions. In addition, the states disperse in a well-behaved manner: their dispersion relations generally follow those of the projected gaps in which they are located.

B. Contamination sensitivity: Chemistry in momentum space

Perhaps the most interesting facet of data such as those presented in Figs. 7 and 8 is the momentum dependence of the sensitivity to contamination. Testing this sensitivity is a standard procedure in ARP experiments to distinguish surface levels. There is, however, much more information available from such data. In essence, in these simple systems we can understand the chemisorption bond momentum by momentum. In this respect, one general though not universal tend observed in our results is that, along both symmetry azimuths, the states which are of predominantly odd symmetry are completely quenched by hydrogen, while those of predominantly even symmetry are simply shifted by typically 0.1–0.3 eV. The nonuniversality of this observation occurs in particular for S_3, a band which exhibits even-polarization behavior but is rapidly attenuated by hydrogen. It is believed that, on W(011), hydrogen adsorbs either into the maximum-coordinate "hourglass" site (i.e., directly above the second layer atoms) or displaced slightly from this site along the [011] direction.[9,16,17,39] If we accept that the same site is preferred on Mo(011), it is difficult to understand the observed enhanced sensitivity of the odd states. The hourglass site is a fully symmetric site, and the hydrogen atom provides an even perturbing potential. One would expect that even-symmetry states would be much more strongly affected by hydrogen adsorption that odd states.

That the reverse is often observed in our data is suggestive that a different adsorption site is preferred on Mo(011). One possibility, the atop site directly above the surface layer, is attractive since that would satisfy the nominal unit valence of the hydrogen atoms. However, this site also is of $2mm$ symmetry and the even states would again be expected to be more sensitive than the odd states. A more likely candidate would be the twofold-coordinated bridge sites. In this position, it can be easily deduced that states of even (odd) symmetry will have reduced (enhanced) amplitude. While the preferential bonding to odd states will not be a symmetry effect as it was for the other sites, we would anticipate enhanced sensitivity of the odd states. We have not developed any intuition as to why this site might be preferred, but the possibility does lead to some interesting conclusions. For instance, the work-function change for hydrogen adsorption on Mo(011) is nearly monotonic and positive,[40] while that for W(011) is just the opposite.[41] The difference in adsorption site would easily explain this apparent enigma, since the hydrogen would be much closer to the surface on tungsten than on molybdenum. Moreover, the bridge site would provide a logical explanation as to why Mo(011) apparently does not reconstruct upon hydrogen adsorption while tungsten does. The simple model of Chung *et al.*[16] only works when the hydrogen is in the hourglass site. Also, the hourglass site puts the hydrogen in a good location to weaken the first- to second-layer bonds, thereby allowing the W(011) surface to reconstruct.[18]

The argument in favor of the bridge site needs to be substantiated by analogous results on W(011), where the opposite contamination sensitivity would be expected if indeed the adsorption site is the hourglass. Our results on W(011) are somewhat more complicated than those on Mo(011).[29] The problem is that the spin-orbit interaction is much larger and the odd-even mixing more pronounced, so that the effects reported here are washed out somewhat. This perhaps provides definitive evidence for the importance of relativistic effects in chemisorption on tungsten. Where identifiably similar bands exist on both surfaces, however, the sensitivity to hydrogen is fairly similar. Further calculations will be required to explain the apparent similarities and difference between these two surfaces.

C. Importance of relativistic effects

Perhaps the most crucial question concerning this work is whether or not these relativistic effects contribute significantly in determining other surface properties. Normally, the spin-orbit interaction affects the total energy of a metal only to fourth order in ξ/W, where W is a representative bandwidth. For small ξ, we expect the spin-orbit interaction not to be too important in determining the lowest-energy geometric arrangement of the surface atoms. It manifests itself more typically in weaker phenomena such as magnetic domain-wall formation. This conclusion is less valid, however, when bands near the Fermi level are strongly perturbed. Indeed, in principle, a metal could be turned into a semiconductor upon introduction of spin-orbit-induced band gaps. In this system, however, all of the hybridization effects we have observed occur away from the Fermi level by several times the spin-orbit parameter. The effect of the spin-orbit interaction on Fermi-surface properties and total energy is probably negligible. For instance, any prediction concerning two-dimensional Fermi-surface nesting and charge-density-wave-driven reconstructions[42–44] will probably not need to consider the spin-orbit interaction in this system. This conclusion will be less true in tungsten, since the analogous eyeball gaps in tungsten lie closer to E_F by ≈ 0.5 eV and the atomic spin-orbit parameter is 3 times larger than in molybdenum. This would indicate that additional fully-relativistic calculations are in order for that metal. It remains to be seen whether this effect can explain the differing reconstructive behavior and work-function change of W(011) and Mo(011) upon hydrogen adsorption.

ACKNOWLEDGMENTS

This work was carried out in part at the National Synchrotron Light Source at Brookhaven National Laboratory, which is supported by the U.S. Department of Energy (DOE), Division of Materials Science and Division of Chemical Sciences. Financial support from the U.S. DOE under Grant No. DE-FG06-86-ER45275 and from the American Chemical Society Petroleum Research Fund is gratefully acknowledged.

[1]E. W. Plummer and W. Eberhardt, *Advances in Chemical Physics* (Wiley, New York, 1982), Vol. 49.
[2]F. J. Himpsel, Adv. Phys. **32**, 1 (1985).
[3]M. Prutton, *Electronic Properties of Surfaces* (Hilger, Bristol, 1984).
[4]M. P. Lopez Sancho, Solid State Commun. **50**, 629 (1984).
[5]P. C. Stephenson and D. W. Bullett, Surf. Sci. **139**, 1 (1985).
[6]R. C. Cinti, E. Al Khoury, B. K. Chakraverty, and N. E. Christensen, Phys. Rev. B **14**, 3296 (1976).
[7]B. Feuerbacher and N. E. Christensen, Phys. Rev. B **10**, 2373 (1974).
[8]M. W. Holmes, D. A. King, and J. E. Inglesfield, Phys. Rev. Lett. **42**, 395 (1979).
[9]G. B. Blanchet, N. J. DiNardo, and E. W. Plummer, Surf. Sci. **118**, 496 (1982).
[10]O. Jepsen and R. O. Jones, Phys. Rev. B **34**, 6695 (1986).
[11]J. P. Bourdin, G. Treglia, M. C. Desjonqueres, J. P. Ganachaud, and D. Spanjaard, Solid State Commun. **47**, 279 (1983).
[12]M. P. Lopez Sancho, J. M. Lopez Sancho, and J. Rubio, J. Phys. C **18**, 1803 (1985).
[13]C. Noguera, D. Spanjaard, and D. W. Jepsen, Phys. Rev. B **17**, 607 (1978).
[14]T. E. Felter, R. A. Barker, and P. J. Estrup, Phys. Rev. Lett. **38**, 1138 (1978).
[15]M. K. Debe and D. A. King, J. Phys. C **10**, L303 (1977).
[16]J. W. Chung, S. C. Ying, and P. J. Estrup, Phys. Rev. Lett. **56**, 749 (1986).
[17]M. Altmann, J. W. Chung, P. J. Estrup, J. M. Kosterlitz, J. Prybyla, D. Sahu, and S. C.Ying, J. Vac. Sci. Technol. **5**, 1045 (1987).
[18]R. H. Gaylord and S. D. Kevan, Phys. Rev. B **37**, 8491 (1988).
[19]F. Herman and S. Skillman, *Atomic Structure Calculations* (Prentice-Hall, Englewood Cliffs, NJ, 1963).
[20]C.-L. Fu and K.-M. Ho, Phys. Rev. B **28**, 5480 (1983).
[21]D. A. Papaconstantopoulos, *Handbook of the Band Structure of Elemental Solids* (Plenum, New York, 1986).
[22]L. F. Matthiess and D. R. Hamann, Phys. Rev. B **29**, 5372 (1984).
[23]R. H. Gaylord and S. D. Kevan, Phys. Rev. B **36**, 9337 (1987).
[24]P. L. Wincott, N. B. Brookes, D. S. Law, and G. Thornton, Phys. Rev. B **33**, 4373 (1986).
[25]G. Jezequel, Y. Petroff, R. Pinchaux, and F. Yndurain, Phys. Rev. B **33**, 4352 (1986).
[26]S. D. Kevan, Rev. Sci. Instrum. **54**, 1441 (1983).
[27]P. Thiry, P. A. Bennett, S. D. Kevan, W. A. Royer, E. E. Chaban, J. E. Rowe, and N. V. Smith, Nucl. Instrum. Methods **222**, 85 (1984).
[28]J. Friedel, P. Lenglart, and G. Leman, J. Phys. Chem. Solids **25**, 781 (1964).
[29]R. H. Gaylord, K. Jeong, and S. D. Kevan (unpublished).
[30]S.-L. Wang, E. W. Plummer, and T. Gustaffson, Phys. Rev. B **18**, 1718 (1978).
[31]K. Jeong, R. H. Gaylord, and S. D. Kevan (unpublished).
[32]S. D. Kevan, N. G. Stoffel, and N. V. Smith, Phys. Rev. B **31**, 1788 (1985).
[33]S. D. Kevan, N. G. Stoffel, and N. V. Smith, Phys. Rev. B **31**, 3348 (1985).
[34]S. D. Kevan and R. H. Gaylord, Phys. Rev. Lett. **57**, 2975 (1986).
[35]S. D. Kevan, Phys. Rev. B **34**, 6713 (1986).
[36]E. T. Goodwin, Proc. Cambridge Philos. Soc. **35**, 205 (1939).
[37]N. V. Smith, Phys. Rev. B **32**, 3549 (1985).
[38]S. L. Hulbert, P. D. Johnson, M. Weinert, and R. F. Garrett, Phys. Rev. B **33**, 760 (1986).
[39]M. Tringedes and R. Gomer, Surf. Sci. **155**, 254 (1985); S. C. Wang and R. Gomer, J. Chem. Phys. **83**, 4193 (1985).
[40]M. L. Ernst-Vidalis, M. Kamaratos, and C. Papageorgopoulos, Surf. Sci. **189**, 276 (1987).
[41]D. D. Barford and R. R. Rye, J. Chem. Phys. **60**, 1046 (1974).
[42]E. Tossatti and P. W. Anderson, Jpn. J. Appl. Phys. Suppl. **2**, Pt. 2, 381 (1974).
[43]J. C. Campuzano, D. A. King, C. Somerton, and J. E. Inglesfield, Phys. Rev. Lett. **45**, 1649 (1980).
[44]J. A. Wilson, F. J. Disalvo, and S. Mahajan, Adv. Phys. **24**, 117 (1975).